

TECHNICAL ADVANCE

A procedure to introduce point mutations into the Rubisco large subunit gene in wild-type plants

Myat T. Lin¹⁺, Douglas J. Orr²⁺, Dawn Worrall², Martin A. J. Parry^{2*}, Elizabete Carmo-Silva²,
Maureen R. Hanson¹

¹ Department of Molecular Biology and Genetics, Cornell University, Ithaca, NY 14850, USA.

² Lancaster Environment Centre, Lancaster University, Library Avenue, Lancaster, LA1 4YQ, UK.

Running title: Introducing point mutations into chloroplast genes

Keywords: chloroplast transformation, food security, homologous recombination, Rubisco, photosynthesis, site-directed mutagenesis, *Nicotiana tabacum*

+ M.T. Lin and D.J. Orr should be considered joint first authors.

*Correspondence: m.parry@lancaster.ac.uk; tel +44 1524 595084

This is the manuscript accepted by the Plant Journal. It was first published online on February 11, 2021 (<https://doi.org/10.1111/tpj.15196>).

SUMMARY

Photosynthetic inefficiencies limit the productivity and sustainability of crop production, and the resilience of agriculture to future societal and environmental challenges. Rubisco is a key target for improvement as it plays a central role in carbon fixation during photosynthesis and is remarkably inefficient. Introduction of mutations to the chloroplast-encoded Rubisco large subunit *rbcL* is of particular interest to improve the catalytic activity and efficiency of the enzyme. However, manipulation of *rbcL* is hampered by its location in the plastome, with many species recalcitrant to plastome transformation, and by the plastid's efficient repair system, which can prevent effective maintenance of mutations introduced with homologous recombination. Here we present a system where the introduction of a number of silent mutations into *rbcL* within the model plant *Nicotiana tabacum* facilitates simplified screening via additional restriction enzyme sites. This system was used to successfully generate a range of transplastomic lines from wild-type *N. tabacum* with stable point mutations within *rbcL* in 40% of the transformants, allowing assessment of the effect of these mutations on Rubisco assembly and activity. With further optimization, the approach offers a viable way forward for mutagenic testing of Rubisco function in planta within tobacco and modifying *rbcL* in other crops where chloroplast transformation is feasible. The transformation strategy could also be applied to introduce point mutations in other chloroplast-encoded genes.

Significance Statement

A simplified transformation strategy was developed to perform site-directed mutagenesis in the chloroplast-encoded Rubisco large subunit of tobacco. This approach reduces unwanted mismatch repair events, enables rapid screening of transformed lines that possess desired mutations and can be applied to modify any chloroplast-encoded gene in plant species amenable to plastid genome transformation.

INTRODUCTION

The transformation of chloroplast or plastid genomes in higher plants represents a promising technology in multiple biotechnological applications such as introducing agronomically important traits, metabolic engineering, recombinant protein expression and production of high-value therapeutic compounds (Maliga and Bock 2011). Chloroplast transformation offers several benefits: precise manipulation of its genome via homologous recombination, no transgene silencing and better control over the transgene escape into the environment. In addition to the introduction and expression of foreign genes, chloroplast transformation can also be used to delete or mutate plastid-encoded protein subunits for functional studies. Since many of these proteins are involved in photosynthesis, the technology has great potential to improve photosynthesis and productivity in crops (Hanson *et al.* 2013, Bock 2015, Martin-Avila *et al.* 2020).

One of the most commonly studied plastid genes is *rbcL*, which encodes the large subunit of ribulose-1,5-bisphosphate carboxylase/oxygenase (Rubisco). In plants, Rubisco catalyses two competing reactions in the stroma of chloroplasts: carboxylation or oxygenation of ribulose-1,5-bisphosphate (RuBP) (Ogren and Bowes 1971, Tcherkez *et al.* 2006, Andersson and Backlund 2008). The carboxylation of RuBP is an essential step for photosynthesis in plants, while its oxygenation generates 2-phosphoglycolate, which is recycled through the photorespiratory pathway, spanning multiple organelles (Ogren and Bowes 1971, Ogren 1984, Keys 1986, Busch 2020). Rubisco in C₃ plants is a relatively slow enzyme with k_{cat} about 3-4 CO₂ s⁻¹ (Orr *et al.* 2016, Flamholz *et al.* 2019). As a result, C₃ plants generally express a large amount of Rubisco within the chloroplast stroma in order to achieve sufficient carbon fixation. Since the reactions of Rubisco control major metabolic fluxes, manipulating its kinetics has been an important target to improve photosynthesis in plants (Sharwood 2017, Zhu *et al.* 2020). Two general goals of engineering Rubisco are to improve its carboxylation efficiency under ambient O₂, which is defined as $k_{\text{cat}}^{\text{C}}/K_{M,\text{air}}^{\text{C}}$, and to increase its CO₂/O₂ specificity factor, which is the ratio of its carboxylation efficiency to oxygenation efficiency or $k_{\text{cat}}^{\text{C}}K_M^{\text{O}}/k_{\text{cat}}^{\text{O}}K_M^{\text{C}}$, where k_{cat} and K_M represent the catalytic turnover number and Michaelis-Menten constant, respectively (Whitney *et al.* 2011a). Increasing Rubisco content in maize and rice led to higher plant biomass,

supporting the hypothesis that Rubisco represents a bottleneck in photosynthesis, and crop yields can be improved with a more efficient Rubisco (Salesse-Smith *et al.* 2018, Yoon *et al.* 2020). However, to date attempts to engineer vascular plants with such a Rubisco enzyme have been unsuccessful.

Rubisco enzymes with different kinetic properties exist in nature despite its well-characterized catalytic constraints (Galmés *et al.* 2015, Galmés *et al.* 2016, Orr *et al.* 2016, Sharwood *et al.* 2016a, Flamholz *et al.* 2019). As organisms adapt to different environments, they have evolved Rubisco enzymes that are optimized to their immediate surroundings (Tcherkez *et al.* 2006, Savir *et al.* 2010). For example, Rubisco in C₄ plants is generally associated with a lower affinity for CO₂ or higher K_M^C and a higher k_{cat}^C compared to those in C₃ plants (Whitney *et al.* 2011a). Modeling studies indicated that a typical C₃ Rubisco is optimized for 220 ppm of atmospheric CO₂ and Rubisco from several C₄ plants would improve carbon fixation in C₃ plants (Zhu *et al.* 2004, Sharwood *et al.* 2016b). Rubisco from red algae such as *Griffithsia monilis* were shown to have the highest known specificity factors and generally assumed to be promising candidates for improving photosynthesis in C₃ plants (Whitney *et al.* 2011a).

Plants possess form I Rubisco, which is a hexadecameric complex made up of eight chloroplast-encoded large subunits (LSu) and eight small subunits (SSu) encoded by a family of *RbcS* nuclear genes and imported to the chloroplast stroma (Whitney *et al.* 2011a). Each holoenzyme complex consists of four LSu dimers with two active sites located inside each dimer at the interface between the two LSu (Andersson and Backlund 2008), and capped with 4 SSu monomers at each end. Plants produce specific chaperonins to prevent irreversible aggregation of LSu as well as multiple chaperones for step-by-step assembly of functional L₈S₈ complexes (Bracher *et al.* 2017, Wilson and Hayer-Hartl 2018). Thus, engineering plants with a more efficient Rubisco that can accumulate the enzyme at sufficiently high levels (Carmo-Silva *et al.* 2015) has been a major challenge.

Engineering Rubisco in higher plants has historically been carried out exclusively in tobacco (*Nicotiana tabacum*), where well-established procedures for chloroplast transformation allowed precise modification of its *rbcL* gene through homologous recombination and, recently, co-engineering of both Rubisco subunits (Sharwood 2017, Martin-Avila *et al.* 2020). Although

LSu from sunflower, Arabidopsis, and C₃ and C₄ Flaveria species were able to assemble with native tobacco SSu to form functional enzymes in tobacco transformant plants, the accumulation of such hybrid enzymes in the leaves was significantly lower than the normal amount, likely due to suboptimal interactions between the foreign LSu and native chaperones or SSu (Kanevski *et al.* 1999, Whitney *et al.* 2011b, Whitney *et al.* 2015). Attempts to replace the *rbcL* gene in tobacco with red algal Rubisco genes produced transformants without functional Rubisco due to incompatibility with the chaperonin machinery and chaperones in tobacco chloroplast stroma (Whitney *et al.* 2001, Lin and Hanson 2018). A recent study demonstrated that a red-type Rubisco from *Rhodobacter sphaeroides* was able to assemble and function in tobacco chloroplasts, but its poor compatibility with native Rubisco activases led to low activation levels in the absence of its cognate Rubisco activase from *Rhodobacter sphaeroides* (Gunn *et al.* 2020). Thus, successfully expressing Rubisco sufficiently distant phylogenetically from the host plant will likely require manipulation of ancillary proteins such as Rubisco activase and/or assembly related factors.

Unless chaperones and SSu can also be optimized to work with a foreign LSu, an alternative approach could be to introduce carefully selected site-directed mutations in the native LSu via chloroplast transformation. However, generating such transformants from wild-type tobacco has been inefficient because the desired mutations introduced by recombination between the mutated *rbcL* and the native version of the gene can be removed by the plastid's repair system before transformants reached homoplasmy (Whitney *et al.* 1999, Kanevski *et al.* 1999). Thus, a tobacco master line has been created where the native *rbcL* gene was replaced with the codon-modified *rbcL* gene from *Rhodospirillum rubrum* with low sequence homology followed by removal of the selectable marker gene to facilitate the introduction of mutated and foreign *rbcL* genes and polycistrons into tobacco (Whitney and Sharwood 2008). This tobacco master line has been successfully used to study the residues critical for the catalytic properties of C₄ Rubisco enzymes in Flaveria species as well as introduction of Arabidopsis LSu into tobacco (Whitney *et al.* 2011b, Whitney *et al.* 2015). In a recent study, inhibiting the expression of native SSu in the tobacco master line with RNA interference allowed the simultaneous transformation of both Rubisco subunits and investigation of the effects of novel Rubisco complexes in tobacco

(Martin-Avila *et al.* 2020). This tobacco master line has been a great resource to carry out Rubisco engineering in a model species, though the generation of such a master line in other plants is a lengthy process, and an efficient procedure to modify chloroplast genes including *rbcL* using a wild-type line would therefore be helpful.

In this study, we developed an approach to effectively introduce specific mutations into chloroplast-encoded genes. As a proof of concept, we synthesized a tobacco *rbcL* gene with synonymous or silent mutations resulting in unique restriction sites. Using this modified *rbcL* gene as a template, we introduced single or double residue substitutions that were predicted in previous phylogenetic and biochemical studies to be potentially important for the enzyme's kinetic properties (Kapralov *et al.* 2012, Galmés *et al.* 2014, Studer *et al.* 2014, Orr *et al.* 2016). This approach allowed us to successfully replace the *rbcL* gene with the modified *rbcL* genes directly within wild-type tobacco plants with high retention of the mutations. A procedure to screen for transformants that possess the mutant *rbcL* genes is described, as well as preliminary analyses of Rubisco activities in ten different transplastomic lines.

RESULTS

Modified restriction sites in the *rbcL* gene allowed efficient screening of the transformants

We synthesized part of a modified *rbcL* gene (*Nt-rbcL^m*) by introducing 26 silent mutations such that four restriction sites were removed while ten were added (Figure 1a, S1). The *Nt-rbcL^m* gene was then seamlessly joined with the native *rbcL* promoter from tobacco and inserted into a chloroplast transformation plasmid, pCT-*rbcL*, described previously (Lin *et al.* 2014). In the resultant chloroplast transformation vector pCT-*Nt-rbcL^m*, the *Nt-rbcL^m* gene followed by the native *rbcL* terminator, Nt-TrbcL, and a selectable marker operon expressing the *aadA* gene driven by the tobacco *psbA* promoter are flanked between a 980 bp upstream homologous region or Flank 1, which contains the native *rbcL* promoter, and a 1kbp downstream homologous region or Flank 2 (Figure 1b). The homologous recombination between the plastid genome and pCT-*Nt-rbcL^m* plasmid through the two flanking regions should introduce the *aadA* marker gene into the plastid genome and facilitate the selection of transformants with

spectinomycin on regeneration medium. However, it is expected that the intended mutations in *Nt-rbcL^m* will be incorporated into only a portion of the transformants with the *aadA* gene. If the cross-over site upstream of the *aadA* gene is located within *Nt-rbcL^m*, the resulting transformants will not possess those mutations upstream of the cross-over site (Figure 1c). Our strategy is to use the unique restriction sites in *Nt-rbcL^m* to screen for the transformants with the intended mutations.

Phylogenetic studies of Rubisco had previously suggested that several amino acid substitutions in LSu were positively selected during the C₃ to C₄ transition (Kapralov *et al.* 2011, Kapralov *et al.* 2012, Studer *et al.* 2014). As detailed in Table 1, we selected five of those mutations (V101I, V255A, L270I, A281S and H282N) and introduced each into the *Nt-rbcL^m* gene as well as a double mutant with both A281S and H282N. We also included the *Nt-rbcL^m* gene with a C449G mutation that was suggested to be associated with improved catalytic efficiency by a previous wide survey of Rubisco kinetic properties from 75 plant species (Orr *et al.* 2016). In addition, we introduced the K429Q mutation to obtain the enzyme from tobacco's paternal parent, *N. tomentosiformis* (accession YP_398871.1). We also created the *Nt-rbcL^m* gene that encodes both K429Q and L225I mutations as the inverse I225L change was found to be selected in evolution of C₃ branches, and ancestors of tobacco Rubisco potentially possessed an L225I mutation (Studer *et al.* 2014).

We introduced each of the pCT-*Nt-rbcL^m* vectors with these mutations into tobacco seedlings of either Samsun or Petit Havana tobacco cultivar with biotics and performed restriction digestion of the PCR-amplified *rbcL* gene from the transformed shoots arising from the first selection round (Figure 2a). We found that typically 40 percent of the shoots at this stage possessed the restriction sites corresponding to the *Nt-rbcL^m* gene. Our result was comparable to that in a previous study, which introduced a different set of silent mutations to remove commonly used restriction sites in the tobacco *rbcL* gene and found that 6 out of 12 or 50% of the transformants had the silent mutations (Sinagawa *et al.* 2009). After the shoots we produced with the modified restriction sites at the *rbcL* locus were subjected to a second round of selection, we analyzed restriction fragment length polymorphisms (RFLPs) in the transformants with DNA blotting (Figure 2b,c). Those transformants that had achieved

homoplasm with the *Nt-rbcL^m* gene were transferred to rooting medium and subsequently to soil until they set seeds. We obtained multiple independent transformants for six out of nine LSu mutations and one each for the remaining three mutations (Table 1). Sequencing of the *rbcL* locus in the final transformants confirmed that all but one of the transformants possessed the entire set of silent mutations in the *Nt-rbcL^m* gene along with the intended non-synonymous mutations. The NtLwt transformant inherited all the silent mutations in the *Nt-rbcL^m* gene minus the single nucleotide change for the new HindIII site (Table 1). Our results are consistent with the previous study which found that the majority, five out of six transformants with silent mutations in the *rbcL* gene, possessed the entire set of mutations and only one originated from a cross-over event within the *rbcL* gene (Sinagawa *et al.* 2009).

Mutations in the Rubisco large subunit did not prevent assembly of Rubisco holoenzyme

We further investigated one tobacco transformant for each Rubisco LSu mutant to determine the effects of the introduced mutations. DNA blotting with a probe hybridized to a region upstream of the *rbcL* gene locus confirmed that all transformants were homoplasmic and possessed a restriction site from the *Nt-rbcL^m* gene (Figure 3). Likewise, an RNA blot of the same samples with a probe to detect the *Nt-rbcL* gene showed that all transformants had an extra dicistronic transcript with both the *Nt-rbcL^m* and downstream *aadA* genes, in addition to the monocistronic *Nt-rbcL^m* transcript (Figure 4a). Both of the *rbcL* transcripts present in the transformants were much less abundant than the single monocistronic transcript from the wild-type sample, however, the total *rbcL* transcript levels in the transformants were comparable to that from the single transcript in the wild-type (Figure 4b). The proportion of dicistronic mRNA amongst the transgenic lines did not significantly vary (ANOVA, P = 0.848). Soluble protein samples from the leaf tissues of the wild-type plant and all transformants displayed a similar band for L₈S₈ holoenzyme on blue native PAGE, indicating these mutations did not prevent Rubisco assembly, though measurements indicate an effect on enzyme abundance in the leaf (Table 2).

Introduced mutations often affected Rubisco carboxylation

To compare the potential impact of these introduced mutations on Rubisco activity an analysis was conducted using glasshouse-grown plants of each transplastomic line and wild-type controls. Leaf discs were taken from 26 day old plants and analysed for maximum Rubisco carboxylation rate (k_{cat}) and other related parameters including total soluble protein and chlorophyll content (Table 2, Table S1). There was significant variation amongst genotypes in the cv. Samsun background (Table 2). Two mutations, V101I and V255A, showed significant negative impact on Rubisco maximum carboxylation rate. Amongst cv. Petit-Havana genotypes there was some evidence for the negative impacts of the C449G mutation, with variation among these genotypes approaching statistical significance ($P = 0.054$, ANOVA). In cv. Petit-Havana genotypes there was also some support for the effect of mutations on Rubisco content and reflected in total soluble protein content (Table 2). Plants of each transplastomic line grew to comparable size and displayed no obvious phenotype under the conditions used (Figure 5). There were no significant differences in chlorophyll content (Table S1). Growth under additional environment conditions will be needed to further explore the effect of the mutations on plant phenotype and enzymatic activity.

DISCUSSION

Engineering the chloroplast genome, or plastome, to utilise the unique characteristics of this organelle is of increasing interest for goals such as improving photosynthesis and the use of plants as bio-factories. The central CO₂ fixing enzyme Rubisco, due its inefficiencies, has long been considered a promising target to improve photosynthesis and increase biomass and yield in crops. Manipulation of Rubisco subunit genes presents contrasting complications. Chloroplast transformation allows precise site-directed mutagenesis of the large subunit (*rbcl*) gene in the chloroplast genome, and although this has long been successfully used to investigate Rubisco biogenesis and biochemistry, the technology is currently limited to a relatively small set of species. Understanding of the pervasive role, in some cases, of the small subunit (encoded by the nuclear RbcS family) on catalysis is rapidly increasing, and despite the complexity of manipulating highly similar gene families, often involving a large number of homologues,

advances are being made in this area (e.g. Martin-Avila *et al.* 2020, Khumsupan *et al.* 2020). In this study, we introduced ten restriction sites with 26 silent mutations in a modified tobacco *rbcL* gene (*Nt-rbcL^m*), which allowed PCR-RFLP screening of transformants after the first round of selection. The elimination of null transformants without the intended mutations after the first selection round also improved the efficiency of workflow to obtain the final stable transformants. Compared to a previous report where only one in eight transformants had the desired mutation in the *rbcL* gene (Whitney *et al.* 1999), about 40 percent of our transformants obtained after the first selection had *Nt-rbcL^m*, with the majority of these giving rise to stable transplastomic plants with the entire set of mutations in the *Nt-rbcL^m* gene. Our results are generally consistent with a previous study to remove common restriction sites in the *rbcL* gene with silent mutations (Sinagawa *et al.* 2009).

It proved useful to generate multiple shoots or subclones from each transformant after the first selection round since more than half of the shoots tested after the second selection round had lost the *Nt-rbcL^m*. This is not surprising since *Nt-rbcL^m* is over 98% identical to the wild-type sequence and can be removed before the transformants reach homoplasmy (Whitney *et al.* 1999, Kanevski *et al.* 1999). There may be potential to further improve the transformation efficiency by increasing the number of silent mutations in *Nt-rbcL^m* such that there is no sequence homology to the wild-type gene. However, having too many silent mutations could possibly interfere with translation efficiency and other underlying sequence-specific regulatory processes, which are not yet fully understood. One such regulatory element that is widely conserved among plants is a major translation pause site within *rbcL* transcripts caused by an internal ribosome-binding site and mRNA structure (Gawroński *et al.* 2018).

Our analyses indicate that many of the transformants with the *Nt-rbcL^m* gene had lower Rubisco content than the wild-type plants although in some cases the difference was not statistically significant. One reason for reduced Rubisco levels could be the 23 modified codons in the *Nt-rbcL^m* gene, with the majority of these changes resulting in the incorporation of less frequently used codons that could negatively impact the protein's translation efficiency. Although translation efficiencies in chloroplasts cannot always be predicted from codon usage and chloroplasts do not possess rare codons similar to those found in *Escherichia coli*, different

codons have varying translation efficiencies so that it may still be desirable to avoid unnecessary codon changes (Nakamura and Sugiura 2011). For example, strategically targetting a single restriction site closest to each non-synonymous mutation instead of introducing the entire set of silent mutations in the *Nt-rbcL^m* gene should minimise unintentional influence on translation efficiencies.

The processing of the *rbcL* mRNA 3' end in our transformants was not efficient, giving rise to a dicistronic transcript with *rbcL* and *aadA* genes. This is likely due to insufficient length of the *rbcL* 3'-UTR, which was 205 nucleotides in the transformants. In addition to the dicistronic transcript, we also observed two sizes for monocistronic mRNAs, indicating a second transcript processing site that is likely in the *psbA* promoter downstream of the *rbcL* 3'-UTR. In a previous study where an *rbcL* 3'-UTR that was 269 nucleotides in length was incorporated downstream of the *rbcL* gene, the dicistronic transcripts were much less abundant, probably due to more efficient processing of the transcripts (Whitney and Sharwood 2008). It was previously shown that 410 nucleotides following *rbcL* was necessary for proper maturation of the *rbcL* transcript (Sinagawa *et al.* 2009). Thus, future work should consider incorporation of a complete *rbcL* 3'-UTR that is at least 410 nucleotides long so that the transformants can produce *rbcL* transcripts that are similar in size and abundance to those in the wild-type. In addition, stem-loop structures at the *loxP* sites flanking the *aadA* operon were suggested to interfere with the processing of both *rbcL* and *aadA* transcripts (Sinagawa *et al.* 2009). Thus, it may be preferable to replace *loxP* sites with long direct repeats that can spontaneously trigger removal of the marker gene through homologous recombination (Iamtham and Day 2000). Alternatively, the marker operon can be flanked with *attB* and *attP* sequences and subsequently removed with the expression of PhiC31 phage integrase (Kittiwongwattana *et al.* 2007).

Previously, the development of a tobacco master line, where the *rbcL* gene had been replaced with a homolog from *Rhodospirillum rubrum* encoding a form II Rubisco, allowed modification of the *rbcL* gene and rapid characterization of the subsequent mutant Rubisco enzymes within 6-9 weeks of transformation, although this master line required a high CO₂ environment to grow in soil (Whitney and Sharwood 2008). Recently, functional Rubisco enzymes from *Arabidopsis* and tobacco were successfully assembled in *Escherichia coli* with the

co-expression of at least five chaperones (Aigner *et al.* 2017, Wilson *et al.* 2019, Lin *et al.* 2020). Thus, modified Rubisco enzymes from plants can now be readily produced in *E. coli*, and once modifications that lead to superior carboxylation kinetics are identified, they can be introduced into host plants for further characterization of their effects on photosynthesis and plant growth. These new tools are complemented by directed evolution approaches with cyanobacterial Rubisco, which have shown promising improvements to catalytic efficiency and specificity (Wilson *et al.* 2018).

As a proof of concept for this approach to mutating chloroplast genes, we generated seven tobacco transformants each with one residue substitution and two transformants each with two residue substitutions in the Rubisco LSu. Most of these residue substitutions were predicted to be selected during the C₃ to C₄ transitions or associated with a higher catalytic efficiency, while L225I and K429Q were potentially present in ancestors of tobacco Rubisco (Studer *et al.* 2014). Mutations that are *bona fide* kinetic switches between C₃ and C₄ Rubisco should result in enzymes with higher k_{cat} (Whitney *et al.* 2011b). However, our analyses indicated a lack of significant improvement in the carboxylation rate of Rubisco from these transformants, indeed a number of the mutant Rubiscos displayed lower maximum carboxylation activities than the control plants. Importantly, the transformants exhibited Rubisco with similar mobility on native PAGE as the wild-type plants, suggesting no impairment of Rubisco biogenesis as a result of the mutations introduced in *rbcL*.

A previous study identified a residue substitution in the Rubisco LSu of *Flaveria* species as a C₃-C₄ kinetic switch, but the same residue substitution which is native to the tobacco enzyme did not convey the same kinetic effect (Whitney *et al.* 2011b). Thus, kinetic switches likely require accessory components, which may be one or more additional complementary mutations in the large or even the small subunit of Rubisco. Indeed, evidence that the residues at the interface between the two subunits play important roles in determining the kinetic properties was previously reported by studies of the Rubisco from *Chlamydomonas* (Spreitzer *et al.* 2005, Genkov and Spreitzer 2009) and cyanobacteria (Wilson *et al.* 2018). Understanding the role of the small subunit in plant Rubisco catalysis is an expanding area, and will be an important complement to engineering the large subunit via chloroplast transformation (e.g.

Ishikawa *et al.* 2011, Morita *et al.* 2014, Atkinson *et al.* 2017, Khumosupan *et al.* 2020), alongside newly developed tools for *rbcL*-*rbcS* co-engineering in the plastome (Martin-Avila *et al.* 2020).

Reliable plastid transformation procedures for many agriculturally important crops are not yet available. A recent study showed that spectinomycin-resistant *Arabidopsis* plastid transformants could be selected with reasonably high efficiency once the nuclear-encoded ACC2, an enzyme subunit involved in fatty acid biosynthesis pathway inside plastids, was knocked out, rendering the plants hypersensitive to spectinomycin (Yu *et al.* 2017). Fertile *Arabidopsis* plastid transformants were then successfully generated when root-derived microcalli of *acc2* knockout lines were used for transformation and regeneration (Ruf *et al.* 2019). These latest developments have potential to inform future attempts to extend plastid transformation technology to other species. Once the plastid genome in crops can be readily transformed, an important goal would be to employ changes within the Rubisco large subunit to improve its properties in key crops such as rice and wheat. Since our approach does not require initial generation of master lines in target plant species, which can be time-intensive, it can greatly expedite future work in introducing targeted changes not only in the Rubisco large subunit, but also in other chloroplast-encoded protein subunits.

EXPERIMENTAL PROCEDURES

Construction of the chloroplast transformation vectors with modified *Nt-rbcL* genes

All primers used were obtained from Integrated DNA Technologies and listed in Table S2. Phusion™ high-fidelity DNA polymerase, FastDigest restriction enzymes and T4 DNA ligase from Thermo Scientific were used to generate amplicons, restriction digests and ligation products respectively. The partial *Nt-rbcL^m* gene (bp172-1362) with silent mutations was synthesized by GenScript and amplified with NtLm-154f and NtLm-1343r primers (Figure 1a, S1). The upstream and downstream fragments were amplified from tobacco DNA with LSU-FL1f+NtLm-171r and NtLm-1363f+NtLrev primers respectively. The three amplicons were joined with overlapping PCR with LSU-FL1f and NtLrev primers, digested with Clal and MauBI and ligated into the similarly digested pCT-*rbcL* vector (described in Lin *et al.* 2014) to obtain pCT-*Nt-rbcL^m* vector

(Figure 1b).

To introduce V101I, L225I, A281S, H282N or A281S/H282N amino-acid substitutions, amplicons obtained with the respective forward primers and NtLrev were digested with *Mlu*I-*Age*I, *Age*I-*Hind*III or *Hind*III-*Not*I and ligated into the similarly digested pCT-Nt-rbcL^m vector. V255A, L270I and C449G mutations were introduced by ligating the amplicons from NtL-97SF and the respective reverse primers into the *Mlu*I-*Sac*I, *Mlu*I-*Hind*III or *Hind*III-*Not*I sites of pCT-Nt-rbcL^m vector. To generate a *Nt-rbcL^m* gene with the K429Q mutation, the two amplicons obtained with NtL-783SF+K429Qr and K429Qf+NtLrev primers were joined with overlapping PCR, digested with *Kpn*I-*Mau*BI and ligated into the similarly digested pCT-Nt-rbcL^m vector. To obtain pCT-Nt-rbcL^m vector with L225I/K429Q mutations, *Nt-rbcL^m* with K429Q was digested with *Kpn*I-*Not*I and ligated into the similarly digested pCT-Nt-rbcL^m-L225I vector. All modified *Nt-rbcL^m* genes were confirmed by Sanger sequencing with NtL-219SR, NtL-97SF and NtL-783SF primers.

Generation of tobacco transformants with modified *Nt-rbcL^m* genes

Each MS agar plate with 25 two-week-old seedlings of either the Samsun or the Petit Havana cultivars of *Nicotiana tabacum* occupying 1 inch² area was bombarded twice with 0.6 µm gold nanoparticles coated with pCT-Nt-rbcL^m vectors in a PDS-1000/He Particle Delivery System (Bio-Rad Laboratories) and the leaf tissues were placed on RMOP agar medium with 500 µg/mL spectinomycin as described previously (Maliga and Tungsuchat-Huang 2014). Five plates of seedlings were bombarded for each transformation vector. The *rbcL* locus was amplified from DNA extracted from the shoots arising from the first selection round with NtL-97SF and NtLrev primers. The amplicons were purified, digested with *Mlu*I, *Age*I or *Hind*III and analyzed on an agarose gel. The shoots possessing the restriction sites in the *rbcL* gene were cut into 25 mm² pieces and placed on RMOP agar medium with 500 µg/mL spectinomycin. After shoots appeared 4-6 weeks later, DNA was extracted from each shoot with CTAB solution (Allen *et al.* 2006), 1 µg each was digested with *Nhe*I and *Xba*I and the RFLP was analyzed on a DNA blot with a DIG-labeled probe as described previously (Orr *et al.* 2020). The shoots homoplasmic with *Nt-rbcL^m* genes were then placed on MS agar medium with 500 µg/mL spectinomycin for

rooting and subsequently transferred to soil. The *Nt-rbcL^m* genes in those plants were confirmed by Sanger sequencing.

Analyses of *Nt-rbcL^m* transcripts in the tobacco transformants

RNA was extracted and purified from young leaves of five-week-old plants with PureLink RNA mini kit from Life Technologies, and 200 ng of each sample was separated in a denaturing gel with 1.3% agarose gel and 2% formaldehyde, transferred to a Nylon membrane and detected with a DIG-labeled RNA probe as described previously (Occhialini *et al.* 2016). The chemiluminescence detection was performed with a ChemiDoc MP imaging system (Bio-Rad) and the band intensities were quantified with Gel Analyzer options in ImageJ software (<https://imagej.nih.gov/ij/>). The experiment was performed for two sets of plants. Five different RNA concentrations (25, 50, 100, 200 and 400 ng) from a wild-type cv. Samsun plant were applied along with each set of samples, and a quadratic function obtained from their band intensities was used to estimate the relative *rbcL* transcript quantity in each band. Each *rbcL* transcript quantity was then normalized with the corresponding 25S rRNA band intensity obtained from the UV exposure of the agarose gel before transfer.

Analyses of Rubisco holoenzyme on blue native PAGE

Leaf tissues were homogenized in an extraction buffer consisting of 100 mM Bicine-NaHO pH 7.9, 5 mM MgCl₂, 1 mM EDTA, 5 mM ϵ -aminocaproic acid, 50 mM 2-mercaptoethanol, 5% (w/v) PEG 4000, 10 mM NaHCO₃, 10 mM DTT and PierceTM protease inhibitor mini tablets (Thermo Scientific part # A32955) and insoluble materials were removed with centrifugation at 16,000 x g at 4°C for 5 min. The protein concentrations were estimated with the Bradford method using a protein assay dye reagent concentrate (Bio-Rad part # 5000006), and 3 μ g of each total soluble extract mixed with a sample buffer consisting of 50 mM BisTris, 50 mM NaCl, 10% w/v glycerol and 0.001% w/v Ponceau S pH 7.2 was loaded to a NativePAGETM 3-12% Bis-Tris protein gel (Thermo Scientific part # BN1003BOX). The electrophoresis was carried out in an XCellTM SureLockTM Mini-Cell with an anode buffer consisting of 50 mM Bis-Tris and 50 mM Tricine pH 6.8 and a cathode buffer consisting of additional 0.002% (w/v) Coomassie G-250 dye at 4°C

150V for 30 min and 250V for ~ 60 min. The gel was fixed with 100 mL of 40% methanol and 10% acetic acid solution for 15-30 min, stained with 100 mL 0.02% Coomassie R-250 in 30% methanol and 10% acetic acid solution for 15-30 min and destained with 100 mL 8% acetic acid solution for 2-5 hours.

Plant material

To obtain plant material for protein analyses, seeds of wild type and transgenic *N. tabacum* cv. Petit Havana and cv. Samsun were sown into planter trays of a commercial potting mix (Petersfield Products, UK) with a slow-release fertiliser (Osmocote, Scotts UK Professional, UK). All lines germinated at similar time post sowing (6 d), and seedlings were thinned out after *ca.* two weeks, with individuals transferred to 1 L pots after *ca.* three weeks. Plants were grown inside a heated glasshouse at Lancaster University, UK, during June-July with minimum day/night temperatures of $25/18 \pm 2^\circ\text{C}$ and a 16 h photoperiod. Supplemental lighting was supplied by sodium lamps when light levels fell below $200 \mu\text{mol m}^{-2} \text{ s}^{-1}$. Plants were kept well-watered.

Protein extraction and analysis

Leaf samples for Rubisco analyses were collected from the youngest fully expanded leaf 32 days after sowing. Samples were collected 3 h after the beginning of the photoperiod, and plants positioned to avoid shading for at least 1 h prior to sampling. Three 0.5 cm^2 leaf discs were rapidly collected using a cork borer and immediately snap frozen, then stored at -80°C prior to analysis.

Frozen leaf samples were homogenised in an ice-cold mortar and pestle in 0.6 mL of extraction buffer, the soluble proteins collected after centrifugation for 1 min at 4°C and $14,700 \times g$, followed immediately by assays of initial and total Rubisco activity, as described by Carmo-Silva *et al.* (2017). Rubisco activation state was calculated as the ratio of initial/total activity. An aliquot (100 μL) of the same soluble protein extract was incubated at RT for 30 mins with 100 μL of CABP binding buffer (Carmo-Silva *et al.* 2017) including [^{14}C]CABP (carboxyarabintol-1,5-bisphosphate), for determination of Rubisco content via [^{14}C]CABP binding (Sharwood *et al.*

2016c).

The same soluble protein extract was used to determine total soluble protein (TSP) via Bradford assay (Bradford 1976). The method of Wintermans and de Mots (1965) was used to determine chlorophyll content, using 20 µL of the homogenate taken in duplicate prior to centrifugation. This was added to 480 µL ethanol, inverted to mix, and kept in the dark for 2-3 h. Absorbance was measured using a SPECTROstar Nano (BMG LabTech, UK) to determine concentrations of chlorophyll a and b.

Statistical analysis

Statistical differences between biochemical trait means were assessed via ANOVA. Where a genotype effect was observed ($P < 0.05$), a post-hoc Tukey's honest significance difference test was used to conduct multiple pairwise comparisons. Analyses were performed using RStudio (version 1.2.5033 (R Studio Team 2019)) and R (version 3.6.2, (R Core Development Team 2013)). Plots were prepared with ggplot2 (Wickham 2016). Outliers were detected using the Tukey's fences method, where outliers are defined as extreme values that are 1.5 times the interquartile range (1.5 IQR) below the first quartile or 1.5 IQR above the third quartile.

Data availability

The data generated in this study can be obtained from the corresponding author upon request.

Accession numbers

Tobacco RbcL sequence data can be found in the GenBank data library under accession number NP_054507.1.

ACKNOWLEDGMENTS

This work was funded by the UK Biotechnology and Biological Sciences Research Council (BBSRC) under grant number BB/I024488/1 to M.A.J.P., the Chemical Sciences, Geosciences, and Biosciences Division, Office of Basic Energy Sciences, Office of Science, U.S. Department of Energy under awards numbers DE-SC0014339 and DE-SC0020142 to M.R.H. and the US National

Science Foundation (NSF) under grant number MCB-1642386 to M.R.H.

List of author contributions:

MTL, MRH, DJO, ECS & MAJP conceived research. MTL, MRH, DJO & ECS designed experiments.

MTL, DJO & DW performed the experiments and analyzed data. All authors contributed to writing the manuscript.

CONFLICTS OF INTEREST

The authors declare that they have no conflicts of interest.

REFERENCES

Aigner, H., Wilson, R.H., Bracher, A., Calisse, L., Bhat, J.Y., Hartl, F.U. and Hayer-Hartl, M. (2017) Plant RuBisCo assembly in *E. coli* with five chloroplast chaperones including BSD2. *Science*, 358, 1272-1278. <https://doi.org/10.1126/science.aap9221>

Allen, G.C., Flores-Vergara, M.A., Krasynanski, S., Kumar, S. and Thompson, W.F. (2006) A modified protocol for rapid DNA isolation from plant tissues using cetyltrimethylammonium bromide. *Nat. Protoc.*, 1, 2320-2325. <https://doi.org/10.1038/nprot.2006.384>

Andersson, I. and Backlund, A. (2008) Structure and function of Rubisco. *Plant Physiol. Biochem.*, 46, 275-291. <https://doi.org/10.1016/j.plaphy.2008.01.001>

Atkinson, N., Leitão, N., Orr, D.J., Meyer, M.T., Carmo-Silva, E., Griffiths, H., Smith, A.M., and McCormick, A.J. (2017). Rubisco small subunits from the unicellular green alga Chlamydomonas complement Rubisco-deficient mutants of *Arabidopsis*. *New Phytol.* 214:655–667.

Bock, R. (2015). Engineering Plastid Genomes: Methods, Tools, and Applications in Basic Research and Biotechnology. *Ann. Rev. Plant. Biol.* 66, 211-241.

Bracher, A., Whitney, S.M., Hartl, F.U. and Hayer-Hartl, M. (2017) Biogenesis and metabolic maintenance of Rubisco. *Annu. Rev. Plant. Biol.*, 68, 29-60. <https://doi.org/10.1146/annurev-arplant-043015-111633>

Bradford, M.M. (1976) A rapid and sensitive method for the quantitation of microgram quantities of protein utilizing the principle of protein-dye binding. *Anal. Biochem.*, 72, 248-254. <https://doi.org/10.1006/abio.1976.9999>

Busch, F.A. (2020) Photorespiration in the context of Rubisco biochemistry, CO₂ diffusion and metabolism. *Plant J.*, 101, 919-939. <https://doi.org/10.1111/tpj.14674>

Carmo-Silva, E., Andralojc, P.J., Scales, J.C., Driever, S.M., Mead, A., Lawson, T., Raines, C.A. and Parry, M.A.J. (2017) Phenotyping of field-grown wheat in the UK highlights contribution of light response of photosynthesis and flag leaf longevity to grain yield. *J. Exp. Bot.*, 68, 3473-3486. <https://doi.org/10.1093/jxb/erx169>

Carmo-Silva, E., Scales, J.C., Madgwick, P.J. and Parry, M.A. (2015) Optimizing Rubisco and its regulation for greater resource use efficiency. *Plant Cell Environ.*, 38, 1817-1832. <https://doi.org/10.1111/pce.12425>

Christin, P.-A., Salamin, N., Muasya, A.M., Roalson, E.H., Russier, F. and Besnard, G. (2008) Evolutionary switch and genetic convergence on *rbcL* following the evolution of C₄ photosynthesis. *Mol. Biol. Evol.*, 25, 2361-2368. <https://doi.org/10.1093/molbev/msn178>

Flamholz, A.I., Prywes, N., Moran, U., Davidi, D., Bar-On, Y.M., Oltrogge, L.M., Alves, R., Savage, D. and Milo, R. (2019) Revisiting trade-offs between Rubisco kinetic parameters. *Biochemistry*, 58, 3365-3376. <https://doi.org/10.1021/acs.biochem.9b00237>

Galmés, J., Hermida-Carrera, C., Laanisto, L. and Niinemets, Ü. (2016) A compendium of temperature responses of Rubisco kinetic traits: variability among and within photosynthetic groups and impacts on photosynthesis modeling. *J. Exp. Bot.*, 67, 5067-5091. <https://doi.org/10.1093/jxb/erw267>

Galmés, J., Kapralov, M.V., Andralojc, P.J., Conesa, M.A., Keys, A.J., Parry, M.A. and Flexas, J. (2014) Expanding knowledge of the Rubisco kinetics variability in plant species: environmental and evolutionary trends. *Plant Cell Environ.*, 37, 1989-2001. <https://doi.org/10.1111/pce.12335>

Galmés, J., Kapralov, M.V., Copolovici, L.O., Hermida-Carrera, C. and Niinemets, Ü. (2015) Temperature responses of the Rubisco maximum carboxylase activity across domains of life: phylogenetic signals, trade-offs, and importance for carbon gain. *Photosynth. Res.*, 123, 183-201. <https://doi.org/10.1007/s11120-014-0067-8>

Gawroński, P., Jensen, P.E., Karpiński, S., Leister, D. and Scharff, L.B. (2018) Pausing of chloroplast ribosomes is induced by multiple features and is linked to the assembly of photosynthetic complexes. *Plant Physiol.*, 176, 2557-2569. <https://doi.org/10.1104/pp.17.01564>

Genkov, T. and Spreitzer, R.J. (2009) Highly conserved small subunit residues influence rubisco large subunit catalysis. *J. Biol. Chem.*, 284, 30105-30112. <https://doi.org/10.1074/jbc.M109.044081>

Gunn, L.H., Martin-Avila, E., Birch, R. and Whitney, S.M. (2020). The dependency of red Rubisco on its cognate activase for enhancing plant photosynthesis and growth. *Proc Nat Acad Sci*, 117, 25890-25896. doi: 10.1073/pnas.2011641117

Hanson, M.R., Gray, B.N. and Ahner, B.A. (2013). Chloroplast transformation for engineering of photosynthesis. *J. Exp. Bot.*, 64, 731–742. <https://doi.org/10.1093/jxb/ers325>

Iamtham, S. and Day, A. (2000) Removal of antibiotic resistance genes from transgenic tobacco plastids. *Nat. Biotechnol.*, 18, 1172-1176. <https://doi.org/10.1038/81161>

Ishikawa, C., Hatanaka, T., Misoo, S., Miyake, C., and Fukayama, H. (2011). Functional incorporation of sorghum small subunit increases the catalytic turnover rate of Rubisco in transgenic rice. *Plant Physiol.*, 156:1603-11.

Kanevski, I., Maliga, P., Rhoades, D.F. and Gutteridge, S. (1999) Plastome engineering of ribulose-1,5-bisphosphate carboxylase/oxygenase in tobacco to form a sunflower large subunit and tobacco small subunit hybrid. *Plant Physiol.*, 119, 133-142. <https://doi.org/10.1104/pp.119.1.133>

Kapralov, M.V. and Filatov, D.A. (2007) Widespread positive selection in the photosynthetic Rubisco enzyme. *BMC Evol. Biol.*, 7, 73. <https://doi.org/10.1186/1471-2148-7-73>

Kapralov, M.V., Kubien, D.S., Andersson, I. and Filatov, D.A. (2011) Changes in Rubisco kinetics during the evolution of C₄ photosynthesis in *Flaveria* (Asteraceae) are associated with positive selection on genes encoding the enzyme. *Mol. Biol. Evol.*, 28, 1491-1503. <https://doi.org/10.1093/molbev/msq335>

Kapralov, M.V., Smith, J.A.C. and Filatov, D.A. (2012) Rubisco evolution in C₄ eudicots: An analysis of Amaranthaceae *Sensu Lato*. *PLoS One*, 7, e52974. <https://doi.org/10.1371/journal.pone.0052974>

Keys, A.J. (1986) Rubisco: its role in photorespiration. *Philos. Trans. R. Soc. Lond. B Biol. Sci.*, 313, 325-336. <https://doi.org/10.1098/rstb.1986.0040>

Khumsupan, P., Kozlowska, M.A., Orr, D.J., Andreou, A.I., Nakayama, N., Patron, N., Carmo-Silva, E. McCormick, A.J. (2020) Generating and characterising single- and multi-gene

mutants of the Rubisco small subunit family in Arabidopsis, *J. Exp. Bot.*, <https://doi.org/10.1093/jxb/eraa316>

Kittiwigwattana, C., Lutz, K., Clark, M. and Maliga, P. (2007) Plastid marker gene excision by the phiC31 phage site-specific recombinase. *Plant Mol. Biol.*, 64, 137-143. <https://doi.org/10.1007/s11103-007-9140-4>

Morita, K., Hatanaka, T., Misoo, S. and Fukayama, H. (2014). Unusual small subunit that is not expressed in photosynthetic cells alters the catalytic properties of Rubisco in rice. *Plant Physiol.*, 164:69–79.

Lin, M.T. and Hanson, M.R. (2018) Red algal Rubisco fails to accumulate in transplastomic tobacco expressing *Griffithsia monilis* *RbcL* and *RbcS* genes. *Plant direct*, 2, e00045. <https://doi.org/10.1002/pld3.45>

Lin, M.T., Occhialini, A., Andralojc, P.J., Parry, M.A. and Hanson, M.R. (2014) A faster Rubisco with potential to increase photosynthesis in crops. *Nature*, 513, 547-550. <https://doi.org/10.1038/nature13776>

Lin, M.T., Stone, W.D., Chaudhari, V. and Hanson, M.R. (2020) Small subunits can determine enzyme kinetics of tobacco Rubisco expressed in *Escherichia coli*. *Nat. Plants* 6, 1289–1299. <https://doi.org/10.1038/s41477-020-00761-5>

Maliga, P. and Bock, R. (2011) Plastid biotechnology: food, fuel, and medicine for the 21st century. *Plant Physiol.*, 155, 1501-1510. <https://doi.org/10.1104/pp.110.170969>

Maliga, P. and Tungsuchat-Huang, T. (2014) Plastid transformation in *Nicotiana tabacum* and *Nicotiana sylvestris* by biolistic DNA delivery to leaves. *Methods Mol. Biol.*, 1132, 147-163. https://doi.org/10.1007/978-1-62703-995-6_8

Martin-Avila, E., Lim, Y.-L., Birch, R., Dirk, L.M.A., Buck, S., Rhodes, T., Sharwood, R.E., Kapralov, M.V. and Whitney, S.M. (2020) Modifying plant photosynthesis and growth via simultaneous chloroplast transformation of Rubisco large and small subunits. *Plant Cell*, 32, 2898-2916. <https://doi.org/10.1105/tpc.20.00288>

Nakamura, M. and Sugiura, M. (2011) Translation efficiencies of synonymous codons for arginine differ dramatically and are not correlated with codon usage in chloroplasts. *Gene*, 472, 50-54. <https://doi.org/10.1016/j.gene.2010.09.008>

Occhialini, A., Lin, M.T., Andralojc, P.J., Hanson, M.R. and Parry, M.A. (2016) Transgenic tobacco plants with improved cyanobacterial Rubisco expression but no extra assembly factors grow at near wild-type rates if provided with elevated CO₂. *Plant J.*, 85, 148-160. <https://doi.org/10.1111/tpj.13098>

Ogren, W.L. (1984) Photorespiration: pathways, regulation, and modification. *Ann. Rev. Plant Physiol.*, 35, 415-442. <https://doi.org/10.1146/annurev.pp.35.060184.002215>

Ogren, W.L. and Bowes, G. (1971) Ribulose diphosphate carboxylase regulates soybean photorespiration. *Nat. New Biol.*, 230, 159-160. <https://doi.org/10.1038/newbio230159a0>

Orr, D.J., Alcantara, A., Kapralov, M.V., Andralojc, P.J., Carmo-Silva, E. and Parry, M.A. (2016) Surveying Rubisco diversity and temperature response to improve crop photosynthetic efficiency. *Plant Physiol.*, 172, 707-717. <https://doi.org/10.1104/pp.16.00750>

Orr, D.J., Worrall, D., Lin, M.T., Carmo-Silva, E., Hanson, M.R. and Parry, M.A.J. (2020) Hybrid cyanobacterial-tobacco Rubisco supports autotrophic growth and procarboxysomal aggregation. *Plant Physiol.*, 182, 807-818. <https://doi.org/10.1104/pp.19.01193>

R Core Development Team (2013) *A language and environment for statistical computing*. <http://www.r-project.org/>.

R Studio Team (2019) *RStudio Cloud: Integrated Development for R*. <https://www.rstudio.com/>.

Ruf, S., Forner, J., Hasse, C., Kroop, X., Seeger, S., Schollbach, L., Schadach, A. and Bock, R. (2019) High-efficiency generation of fertile transplastomic *Arabidopsis* plants. *Nat. Plants*, 5, 282-289. <https://doi.org/10.1038/s41477-019-0359-2>

Salesse-Smith, C.E., Sharwood, R.E., Busch, F.A., Kromdijk, J., Bardal, V. and Stern, D.B. (2018) Overexpression of Rubisco subunits with RAF1 increases Rubisco content in maize. *Nat. Plants*, 4, 802-810. <https://doi.org/10.1038/s41477-018-0252-4>

Savir, Y., Noor, E., Milo, R. and Tlusty, T. (2010) Cross-species analysis traces adaptation of Rubisco toward optimality in a low-dimensional landscape. *Proc. Natl. Acad. Sci. U. S. A.*, 107, 3475-3480. <https://doi.org/10.1073/pnas.0911663107>

Sharwood, R.E. (2017) Engineering chloroplasts to improve Rubisco catalysis: prospects for translating improvements into food and fiber crops. *New Phytol.*, 213, 494-510. <https://doi.org/10.1111/nph.14351>

Sharwood, R.E., Ghannoum, O., Kapralov, M.V., Gunn, L.H. and Whitney, S.M. (2016a) Temperature responses of Rubisco from Paniceae grasses provide opportunities for improving C₃ photosynthesis. *Nat. Plants*, 2, 16186. <https://doi.org/10.1038/nplants.2016.186>

Sharwood, R.E., Ghannoum, O. and Whitney, S.M. (2016b) Prospects for improving CO₂ fixation in C₃-crops through understanding C₄-Rubisco biogenesis and catalytic diversity. *Curr. Opin. Plant Biol.*, 31, 135-142. <https://doi.org/10.1016/j.pbi.2016.04.002>

Sharwood, R.E., Sonawane, B.V., Ghannoum, O. and Whitney, S.M. (2016c) Improved analysis of C₄ and C₃ photosynthesis via refined *in vitro* assays of their carbon fixation biochemistry. *J. Exp. Bot.*, 67, 3137-3148. <https://doi.org/10.1093/jxb/erw154>

Sinagawa-García, S.R., Tungsuchat-Huang, T., Paredes-López, O. and Maliga, P. (2009) Next generation synthetic vectors for transformation of the plastid genome of higher plants. *Plant Mol. Biol.*, 70, 487-498. <https://doi.org/10.1007/s11103-009-9486-x>

Spreitzer, R.J., Peddi, S.R. and Satagopan, S. (2005) Phylogenetic engineering at an interface between large and small subunits imparts land-plant kinetic properties to algal Rubisco. *Proc. Natl. Acad. Sci. U. S. A.*, 102, 17225-17230. <https://doi.org/10.1073/pnas.0508042102>

Studer, R.A., Christin, P.A., Williams, M.A. and Orengo, C.A. (2014) Stability-activity tradeoffs constrain the adaptive evolution of RubisCO. *Proc. Natl. Acad. Sci. U. S. A.*, 111, 2223-2228. <https://doi.org/10.1073/pnas.1310811111>

Tcherkez, G.G.B., Farquhar, G.D. and Andrews, T.J. (2006) Despite slow catalysis and confused substrate specificity, all ribulose bisphosphate carboxylases may be nearly perfectly optimized. *Proc. Natl. Acad. Sci. U. S. A.*, 103, 7246-7251. <https://doi.org/10.1073/pnas.0600605103>

Whitney, S.M., Baldet, P., Hudson, G.S. and Andrews, T.J. (2001) Form I Rubiscos from non-green algae are expressed abundantly but not assembled in tobacco chloroplasts. *Plant J.*, 26, 535-547. <https://doi.org/10.1046/j.1365-313x.2001.01056.x>

Whitney, S.M., Birch, R., Kelso, C., Beck, J.L. and Kapralov, M.V. (2015) Improving recombinant Rubisco biogenesis, plant photosynthesis and growth by coexpressing its ancillary RAF1 chaperone. *Proc. Natl. Acad. Sci. U. S. A.*, 112, 3564-3569.
<https://doi.org/10.1073/pnas.1420536112>

Whitney, S.M., Houtz, R.L. and Alonso, H. (2011a) Advancing our understanding and capacity to engineer nature's CO₂-sequestering enzyme, Rubisco. *Plant Physiol.*, 155, 27-35.
<https://doi.org/10.1104/pp.110.164814>

Whitney, S.M. and Sharwood, R.E. (2008) Construction of a tobacco master line to improve Rubisco engineering in chloroplasts. *J. Exp. Bot.*, 59, 1909-1921.
<https://doi.org/10.1093/jxb/erm311>

Whitney, S.M., Sharwood, R.E., Orr, D., White, S.J., Alonso, H. and Galmes, J. (2011b) Isoleucine 309 acts as a C₄ catalytic switch that increases ribulose-1,5-bisphosphate carboxylase/oxygenase (rubisco) carboxylation rate in *Flaveria*. *Proceedings of the National Academy of Sciences*, 108, 14688-14693.
<https://doi.org/10.1073/pnas.1109503108>

Whitney, S.M., von Caemmerer, S., Hudson, G.S. and Andrews, T.J. (1999) Directed mutation of the Rubisco large subunit of tobacco influences photorespiration and growth. *Plant Physiol.*, 121, 579-588. <https://doi.org/10.1104/pp.121.2.579>

Wickham, H. (2016) *ggplot2: Elegant Graphics for Data Analysis Using the Grammar of Graphics* New York: Springer-Verlag.

Wilson, R.H. and Hayer-Hartl, M. (2018) Complex chaperone dependence of Rubisco biogenesis. *Biochemistry*, 57, 3210-3216. <https://doi.org/10.1021/acs.biochem.8b00132>

Wilson, R. H., Martin-Avila, E., Conlan, C. and Whitney, S.M. (2018) An improved Escherichia coli screen for Rubisco identifies a protein-protein interface that can enhance CO₂-fixation kinetics. *Journal of Biological Chemistry*. 293, 18-27. doi: 10.1074/jbc.M117.810861.

Wilson, R.H., Thieulin-Pardo, G., Hartl, F.U. and Hayer-Hartl, M. (2019) Improved recombinant expression and purification of functional plant Rubisco. *FEBS Lett.*, 593, 611-621.
<https://doi.org/10.1002/1873-3468.13352>

Wintermans, J.F. and de Mots, A. (1965) Spectrophotometric characteristics of chlorophylls *a* and *b* and their pheophytins in ethanol. *Biochim. Biophys. Acta*, 109, 448-453.
[https://doi.org/10.1016/0926-6585\(65\)90170-6](https://doi.org/10.1016/0926-6585(65)90170-6)

Yoon, D.-K., Ishiyama, K., Suganami, M., Tazoe, Y., Watanabe, M., Imaruoka, S., Ogura, M., Ishida, H., Suzuki, Y., Obara, M., Mae, T. and Makino, A. (2020) Transgenic rice overproducing Rubisco exhibits increased yields with improved nitrogen-use efficiency in an experimental paddy field. *Nat. Food*, 1, 134-139. <https://doi.org/10.1038/s43016-020-0033-x>

Yu, Q., Lutz, K.A. and Maliga, P. (2017) Efficient plastid transformation in *Arabidopsis*. *Plant Physiol.*, 175, 186-193. <https://doi.org/10.1104/pp.17.00857>

Zhu, X.G., Ort, D.R., Parry, M. and von Caemmerer, S. (2020) A wish list for synthetic biology in photosynthesis research. *J. Exp. Bot.* <https://doi.org/10.1093/jxb/eraa075>

Zhu, X.G., Portis, A.R. and Long, S.P. (2004) Would transformation of C₃ crop plants with foreign Rubisco increase productivity? A computational analysis extrapolating from kinetic

properties to canopy photosynthesis. *Plant Cell Environ.*, 27, 155-165.
<https://doi.org/10.1046/j.1365-3040.2004.01142.x>

Table 1. Summary on the generation of tobacco chloroplast transformants with point mutations in the Rubisco large subunit and the number of independent shoots obtained at each step of selection.

Cultivar	Mutations	Predicted roles and references	Number of independent shoots obtained at each stage of selection			
			1 st round	1 st round with expected restriction fragments	homoplasmic shoots after the 2 nd selection round	Final independent transformants
Samsun	None (NtLwt)	Unmodified Rubisco	8	2	1	1*
Samsun	V101I	C ₃ to C ₄ transition (Christin <i>et al.</i> 2008, Studer <i>et al.</i> 2014)	2	1	1	1
Samsun	V255A	C ₃ to C ₄ transition (Studer <i>et al.</i> 2014, Christin <i>et al.</i> 2008, Kapralov and Filatov 2007)	4	1	1	1
Samsun	A281S	C ₃ to C ₄ transition (Christin <i>et al.</i> 2008, Studer <i>et al.</i> 2014)	8	3	3	3
Samsun	H282N	C ₃ to C ₄ transition (Studer <i>et al.</i> 2014)	5	3	3	3
Samsun	A281S,H282N	See A281S and H282N above	4	2	2	2
Petit Havana	L270I	C ₃ to C ₄ transition (Christin <i>et al.</i> 2008, Studer <i>et al.</i> 2014)	7	4	3	3
Petit Havana	L225I, K429Q	C ₃ branch for L225I (Studer <i>et al.</i> 2014, Kapralov and Filatov 2007)	5	2	2	2
Petit Havana	K429Q	Found in paternal parent (<i>N. tomentosiformis</i>)	4	3	3	2
Petit Havana	C449G	Improved catalytic efficiency (Orr <i>et al.</i> 2016)	3	1	1	1

* The NtLwt transformant possesses all the silent mutations in the *Nt-rbcL^m* gene except for a single mutation necessary for the new HindIII site. All the other transformants have the entire set of silent mutations in the *Nt-rbcL^m* gene as well as the intended non-synonymous mutations.

Table 2. Rubisco carboxylation rate (k_{cat}), content and total soluble protein (TSP) of transplastomic tobacco producing Rubisco with mutations in the large subunit. Transplastomic lines were compared statistically with the respective wild-type background. Values represent mean \pm S.E. (n = 3-6 replicate plants), letters denote significant differences (p < 0.05) as determined by Tukey's pairwise comparisons following ANOVA.

Genotype	Rubisco k_{cat} (s^{-1})	Rubisco ($\mu\text{mol sites m}^{-2}$)	TSP (g m^{-2})	TSP (% Rubisco)	Activation state (%)
WT-SS	2.6 ^a \pm 0.2	24.6 \pm 2.8	4.8 \pm 0.5	36.2 \pm 2.7	82.4 \pm 2.6
NtLwt	2.4 ^{ab} \pm 0.2	18.6 \pm 2.5	4.0 \pm 0.7	36.0 \pm 4.6	78.0 \pm 2.9
V101I	1.6 ^b \pm 0.1	19.5 \pm 1.1	4.7 \pm 0.1	29.1 \pm 1.3	71.2 \pm 6.2
V255A	1.6 ^b \pm 0.0	18.2 \pm 2.9	3.7 \pm 0.2	34.1 \pm 3.1	69.4 \pm 5.9
A281S	1.8 ^{ab} \pm 0.2	17.8 \pm 2.7	3.5 \pm 0.3	35.4 \pm 4.3	74.4 \pm 5.1
H282N	2.2 ^{ab} \pm 0.3	15.3 \pm 2.8	3.2 \pm 0.2	33.6 \pm 4.4	71.1 \pm 4.5
A281S/H282N	2.1 ^{ab} \pm 0.2	18.9 \pm 3.3	3.5 \pm 0.3	37.2 \pm 3.8	72.4 \pm 2.1
<i>P</i> = 0.007		= 0.337	= 0.249	= 0.842	= 0.216
Genotype	Rubisco k_{cat} (s^{-1})	Rubisco ($\mu\text{mol sites m}^{-2}$)	TSP (g m^{-2})	TSP (% Rubisco)	Activation state (%)
WT-PH	2.5 \pm 0.2	26.6 ^a \pm 1.3	5.6 ^a \pm 0.4	33.9 \pm 2.5	71.1 \pm 2.5
C449G	1.5 \pm 0.2	22.1 ^{ab} \pm 4.2	5.2 ^{ab} \pm 0.5	29.3 \pm 3.2	68.3 \pm 1.9
K429Q	1.9 \pm 0.1	19.7 ^{ab} \pm 2.2	5.0 ^{ab} \pm 0.6	28.0 \pm 2.6	68.4 \pm 2.8
L225I/K429Q	2.4 \pm 0.3	15.1 ^b \pm 0.7	3.2 ^b \pm 0.6	35.6 \pm 6.7	83.6 \pm 4.5
L270I	1.9 \pm 0.2	19.3 ^{ab} \pm 2.4	4.4 ^{ab} \pm 0.3	30.9 \pm 3.3	74.7 \pm 3.9
<i>P</i> = 0.054		= 0.018	= 0.025	= 0.612	= 0.165

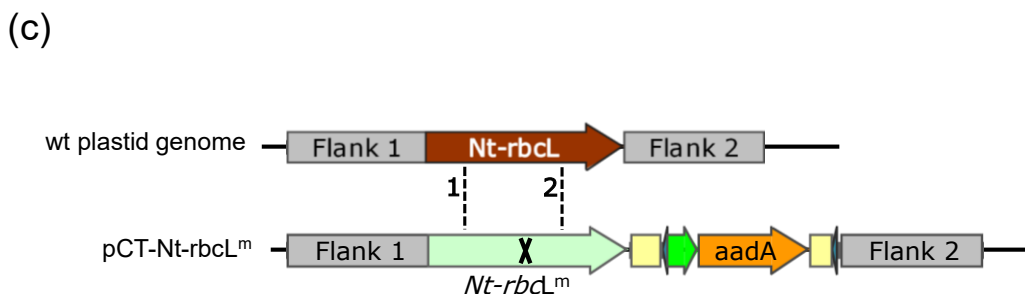
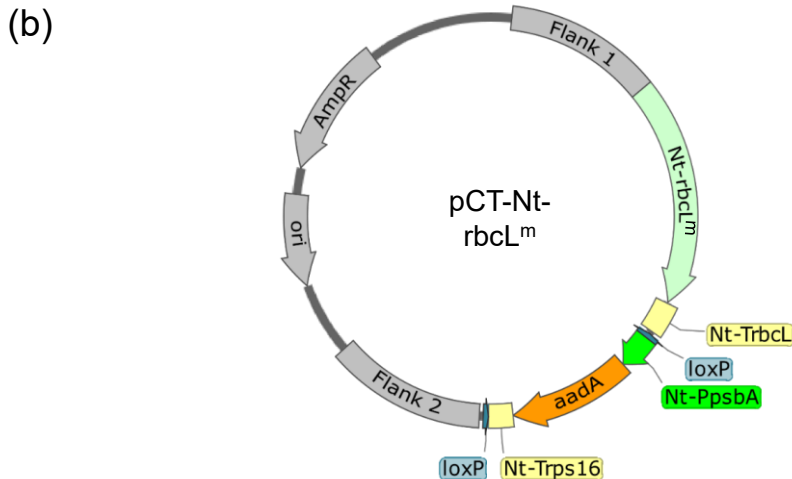
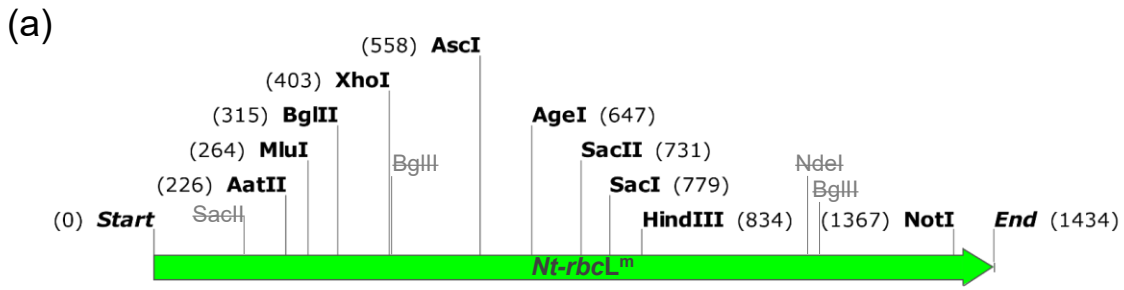
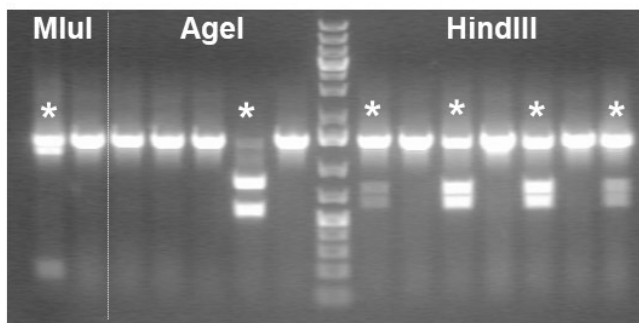
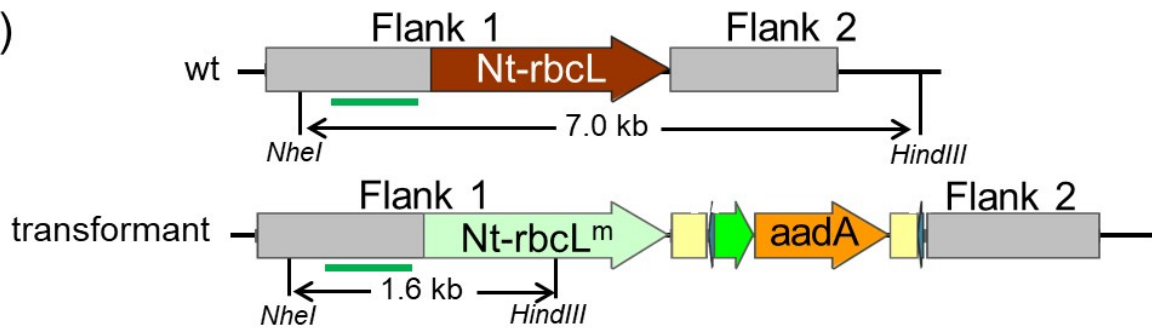


Figure 1. Modification of the tobacco *rbcL* gene for chloroplast transformation. (a) Schematic diagrams of the synthesized *Nt-rbcL^m* gene with modified restriction sites. (b) The chloroplast transformation vector pCT-*Nt-rbcL^m* for replacing the tobacco *rbcL* gene with *Nt-rbcL^m*. (c) Comparison of two hypothetical scenarios of cross-over events between the *rbcL* locus of the plastid genome and pCT-*Nt-rbcL^m* plasmid upstream of the selectable marker *aadA* gene. The location of a hypothetical point mutation in *Nt-rbcL^m* gene on pCT-*Nt-rbcL^m* plasmid is indicated with an 'X'. The two cross-over events are indicated with dashed lines between the plastid genome and pCT-*Nt-rbcL^m* plasmid. If the cross-over takes place in Flank 1 or inside *Nt-rbcL^m* upstream of 'X' as in event 1, the point mutation will be introduced into the transformant. On the other hand, the cross-over taking place downstream of 'X' will fail to introduce the point mutation into the transformant. Note that although the segment upstream of *Nt-rbcL* has been marked as "Flank 1", *Nt-rbcL* should be considered as part of Flank 1 due to high homology between *Nt-rbcL* and *Nt-rbcL^m*.

(a)



(b)



(c)

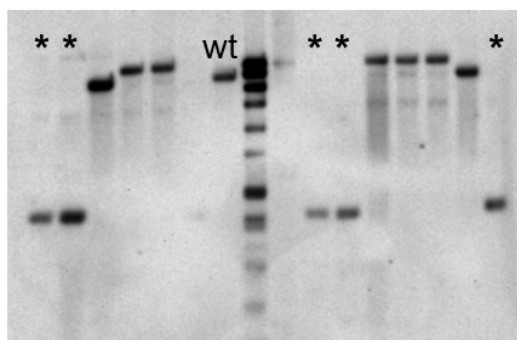
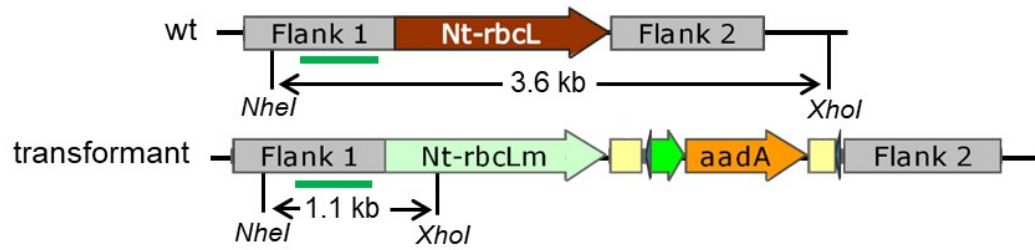


Figure 2. Selection of tobacco transformants with the *Nt-rbcL^m* gene. (a) Restriction analyses of the amplified *rbcL* locus from tobacco transformants after the first selection round. The examples shown include *Mlu*I, *Age*I and *Hind*III digests of transformants with V101I, H282N and A281S/H282N mutations respectively. The samples with digestion fragments expected for *Nt-rbcL^m* are indicated with asterisks (*). (b) Schematics of the *rbcL* loci of the wild-type and *Nt-rbcL^m* transformants with the restriction sites used in DNA blot analyses. The green bars represent the region where the probe binds. (c) DNA blot analyses of tobacco transformants with *Nt-rbcL^m*. The samples with successful replacement of the native *rbcL* gene with *Nt-rbcL^m* are indicated with asterisks (*).

(a)



(b)

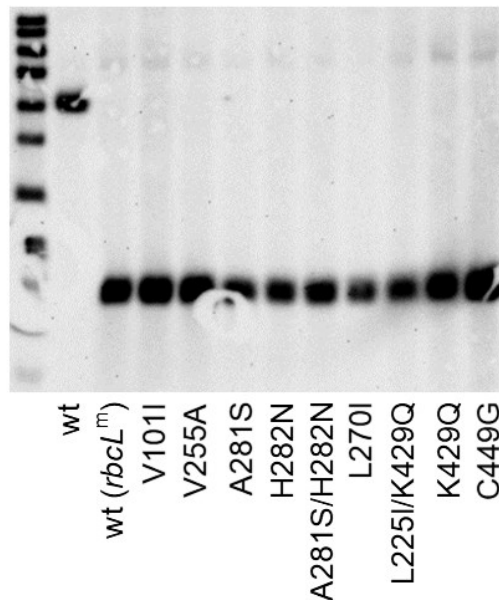


Figure 3. DNA blot analyses of the tobacco chloroplast transformants with *Nt-rbcL^m* gene encoding Rubisco large subunit mutants. (a) Schematics of the the *rbcL* loci of the wild-type (wt) and *Nt-rbcL^m* transformants with the restriction sites used in DNA blot analyses. The green bars represent the region where the probe binds. (b) DNA blot indicating successful replacement of the native *rbcL* gene with *Nt-rbcL^m* in the transformants.

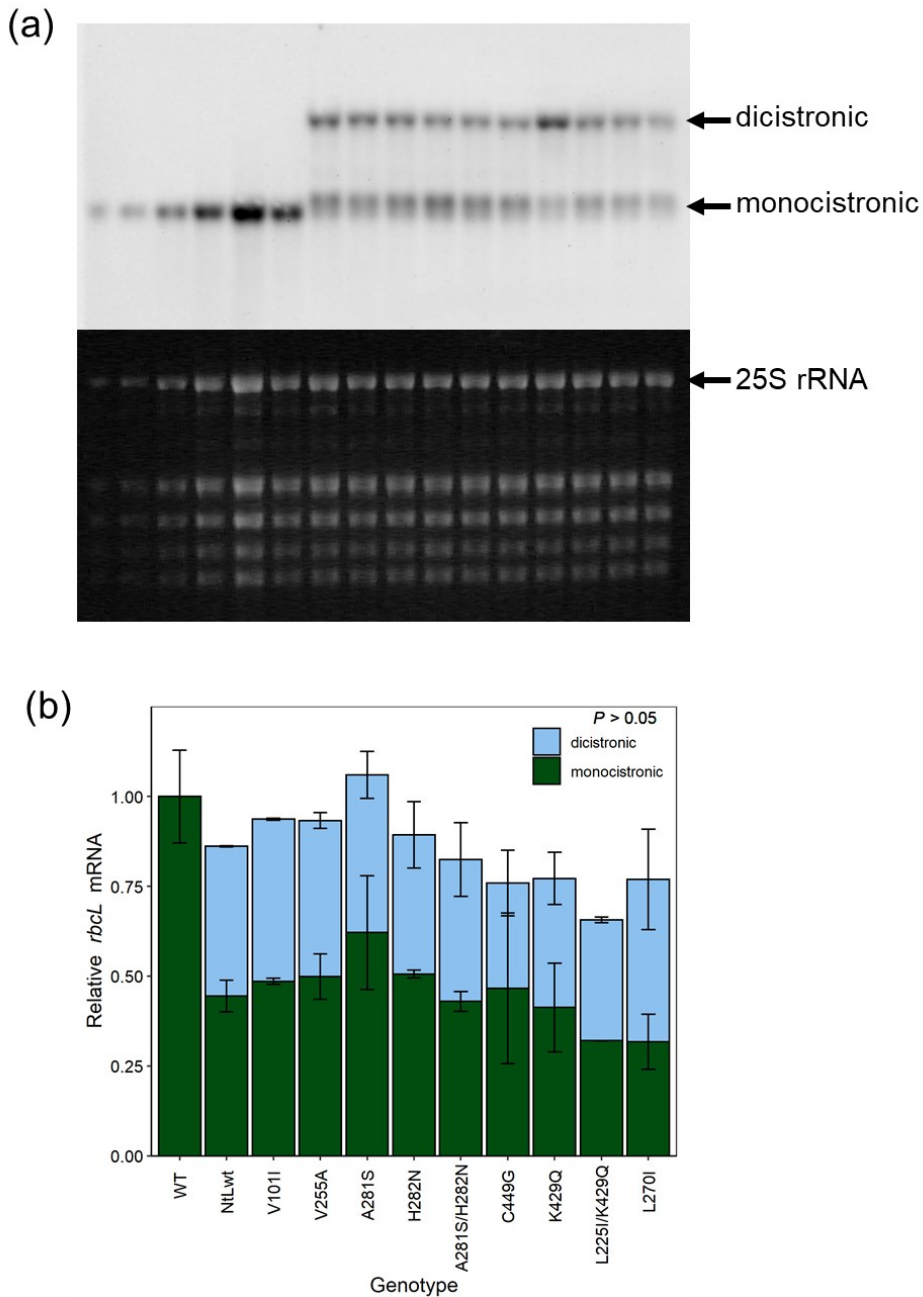


Figure 4. RNA blot analyses of the *rbcL* transcripts in tobacco transformants with *Nt-rbcL^m* encoding Rubisco large subunit mutants. (a) The RNA blot for *rbcL* transcripts in the wt (left six lanes and transformants (right ten lanes). In addition to the monocistronic *rbcL* transcript, all transformants display an additional dicistronic transcript with *rbcL* and *aadA* genes. The bottom panel shows ethidium bromide staining of the agarose gel. 25S rRNA band was used to estimate the relative amounts of total RNA loaded for each sample. The transformants are in the same order as in (b). (b) The relative quantities of *rbcL* transcripts in the transformants compared to that in the wild-type plants obtained from two sets of plants. P values were determined by Tukey's pairwise comparisons following ANOVA.

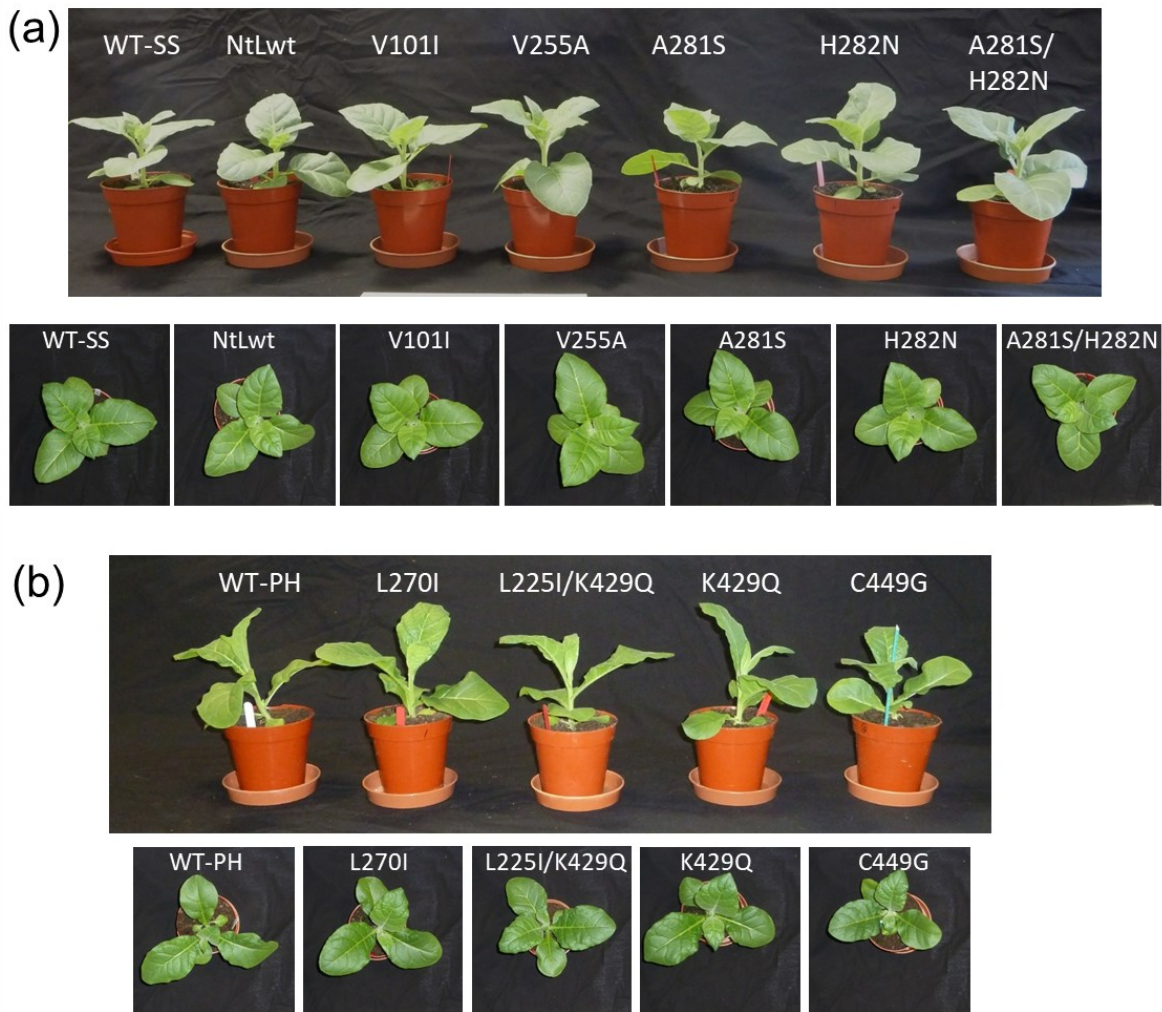
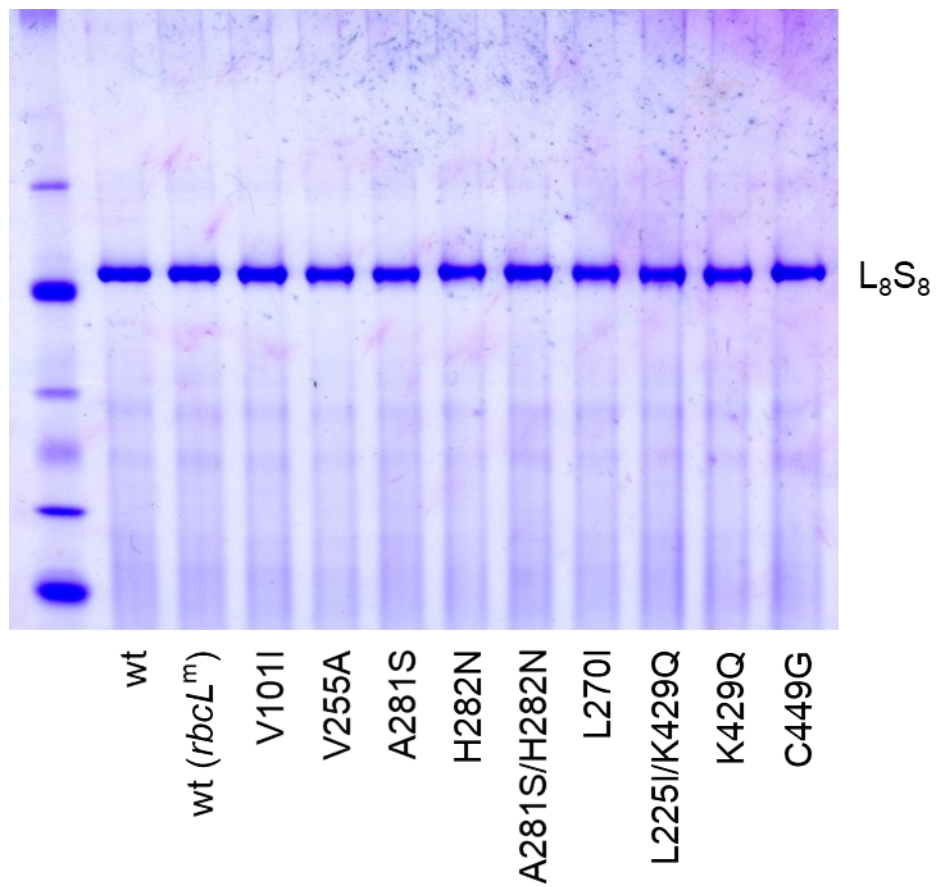


Figure 5. Visual comparison of plant development. (a) wild-type tobacco cv. Samsun (WT-SS) and *rbcL* transplastomic lines, and (b) wild-type tobacco cv. Petite Havana (WT-PH) and *rbcL* transplastomic lines. Photos were taken of plants at the same age (35 days after sowing) and growth stage.

57600	ATGTCACCACAAACAGAGACTAAAGCAAGTGTGGATTCAAAGCTGGTAAAGAGTAC	57659
1	60
57660	AAATTGACTTATTATACTCCTGAGTACCAACCAAGGATACTGATATATTGGCAGCATTC	57719
61	120
57720	CGAGTAACCTCAACCTGGAGTTCCACCTGAAGAAGCAGGGGCCGGTAGCTGCCAA	57779
121 A	180
57780	TCTTCTACTGGTACATGGACAACGTGATGGACCGATGGACTTACCAAGCCTGATCGTTAC	57839
181 G .. GTC	240
57840	AAAGGGCGATGCTACCGCATCGAGCGTGTGTTGGAGAAAAAGATCAATATATTGCTTAT	57899
241 A .. C	300
57900	GTAGCTTACCCCTTAGACCTTTGAAGAAGGTTCTGTTACCAACATGTTACTTCCATT	57959
301 T	360
57960	GTAGGTAACGTATTTGGGTTCAAAGCCCTGCGCCTACGTCTGGAAAGATCTGCGAATC	58019
361 C .. G	420
58020	CCTCCTGCTTATGTTAAAACTTCCAAGGTCCGCCTCATGGGATCCAAGTTGAAAGAGAT	58079
421	480
58080	AAATTGAACAAGTATGGTCGTCCCCTGTTGGGATGTACTATTAAACCTAAATTGGGTTA	58139
481	540
58140	TCTGCTAAAAACTACGGTAGAGCTGTTATGAATGTCCTCGCGGTGACTTGATTTAC	58199
541 GC .. C .. C	600
58200	AAAGATGATGAGAACGTGAACCTACAACCATTATGCGTTGGAGAGATCGTTCTTATT	58259
601 C .. G	660
58260	TGTGCCGAAGCACTTATAAAGCACAGGCTGAAACAGGTGAAATCAAAGGGCATTACTTG	58319
661	720
58320	AATGCTACTGCAGGTACATGCGAAGAAATGATCAAAGAGCTGTATTGCTAGAGAATTG	58379
721 C .. G GC .. C	780
58380	GGCGTTCGATCGTAATGCATGACTACTTAACGGGGATTACCGCAAATACTAGCTTG	58439
781 A	840
58440	GCTCATTATTGCCGAGATAATGGCTACTTCTTCACATCCACCGTGCAATGCATCGGTT	58499
841	900
58500	ATTGATAGACAGAAGAACATGGTATCCACTCCGGTATTAGCAAAGCGTTACGTATG	58559
901	960
58560	TCTGGTGGAGATCATATTCACTCTGGTACCGTAGTAGGTAACCTGAAGGTGAAAGAGAC	58619
961	1020
58620	ATAACTTGGGCTTGTGATTACTGCGTGATGATTGTTGAACAAGATCGAAGTCGC	58679
1021	1080
58680	GGTATTATTCACTCAAGATTGGGCTCTTACCAAGGTGTTCTACCGTGGCTTCAGGA	58739
1081	1140
58740	GGTATTCACTGGCATATGCCTGCTGACCGAGATCTTGGGATGATTCCGTACTA	58799
1141 C A	1200
58800	CAGTCGGTGGAGGAACCTAGGACATCCTGGGTAATGCGCCAGGTGCGTAGCTAAT	58859
1201	1260
58860	CGAGTAGCTCTAGAACATGTGAAAGCTCGTAATGAAGGACGTGATCTGCTCAGGAA	58919
1261	1320
58920	GGTAATGAAATTATCGCGAGGCTTGCAAATGGAGCCGGAACTAGCTGCTGCTGTGAA	58979
1321 G .. C	1380
58980	GTATGGAAAGAGATCGTATTAATTTCAGCAGTGGACGTTGGATAAGTAA	59033
1381	1434

Supplemental Figure S1. Sequence alignment of the tobacco *rbcL* gene open reading frame from chloroplast genome (Accession: NC_001879.2, top) and the synthesized *Nt-rbcL^m* (bottom) using blastn program (<https://blast.ncbi.nlm.nih.gov/Blast.cgi?PROGRAM=blastn>). Numbers indicate position within *N. tabacum* plastome (top line) and synthesized *Nt-rbcL^m* (bottom line).



Supplemental Figure S2. Blue native PAGE analyses of soluble protein extracts from young leaves of tobacco transformants with *Nt-rbcL*^m encoding Rubisco large subunit mutants. Approximately 3 μ g of total soluble extract was loaded for each sample. The gel was stained with Coomassie blue R-250.

Supplemental Table S1. Chlorophyll data from analysis of tobacco transplastomic lines. Data were determined from the same samples as those used for protein biochemistry (Table 2). Transplastomic lines were compared statistically with the respective wild-type background. Values represent mean \pm S.E. (n = 3-6 replicate plants). Letters denote significant differences (p < 0.05) as determined by Tukey's pairwise comparisons following ANOVA (p-values are indicated for each trait, and bolded where p < 0.05).

Genotype	Chlorophyll a (mg m ⁻²)	Chlorophyll b (mg m ⁻²)	Total chlorophyll (mg m ⁻²)	Chlorophyll a/b
WT-SS	304 \pm 32	127 \pm 13	431 \pm 45	2.40 \pm 0.03
NtLwt	282 \pm 26	118 \pm 11	401 \pm 37	2.38 \pm 0.03
V101I	418 \pm 24	178 \pm 13	596 \pm 36	2.35 \pm 0.05
V255A	350 \pm 77	157 \pm 37	506 \pm 114	2.25 \pm 0.04
A281S	305 \pm 67	133 \pm 29	438 \pm 95	2.29 \pm 0.03
H282N	252 \pm 80	110 \pm 36	362 \pm 115	2.30 \pm 0.02
A281S/H282N	359 \pm 19	156 \pm 9	515 \pm 28	2.31 \pm 0.03
<i>P</i>	= 0.387	= 0.388	= 0.389	= 0.057
Genotype	Chlorophyll a (mg m ⁻²)	Chlorophyll b (mg m ⁻²)	Total chlorophyll (mg m ⁻²)	Chlorophyll a/b
WT-PH	366 \pm 41	147 \pm 16	513 \pm 57	2.49 ^a \pm 0.02
C449G	392 \pm 70	167 \pm 32	560 \pm 102	2.35 ^{ab} \pm 0.05
K429Q	399 \pm 75	168 \pm 33	567 \pm 107	2.39 ^{ab} \pm 0.03
L225I/K429Q	348 \pm 54	149 \pm 23	497 \pm 77	2.34 ^b \pm 0.01
L270I	391 \pm 73	167 \pm 32	558 \pm 105	2.35 ^b \pm 0.05
<i>P</i>	= 0.977	= 0.946	= 0.971	= 0.022

Supplemental Table S2. Oligonucleotide sequences used in the construction of transformation vectors

Names	Sequences (5' to 3')
NtLm-154f	GAAGCAGGGGCAGCGGTAGCTGCCGAATCTCTACTGGTAC
NtLm-1343r	CTTCACAAGCGGCCGCTAGTCCGGGCTCCATTGCAAG
LSU-FL1f	CACTATCTGACCTTGAAC
NtLm-171r	TACCGCTGCCCTGCTTCTTC
NtLm-1363f	CTAGCGGCCGCTTGTGAAGTATG
NtLrev	AGATCGCGCGCTTACTTATCCAAAACGTCCACTGC
NtL-219SR	TCCATCGGTCCATACAGTTG
NtL-97SF	GATACTGATATATTGGCAGCATT
NtL-783SF	CGTTCCGATCGTAATGCATG
V101If	TCGAACGCGTTGTTGGAGAAAAGATCAATATATTGCTTAT <u>A</u> TAGCTTACCCTTAG
L225If	AGAGACCGGTTCTTATTGTGCCGAAG <u>C</u> A <u>T</u> TTATAAAGCACAG
V255Ar	AGATGAGCTCTCTAGCAAAT <u>G</u> CAGCTTTGATCATTC
L270Ir	AGATAAGCTTGTATTGCGGTGAATCCCCCGTT <u>T</u> GTAGTCATGCATTACGATC
A281Sf	ATACAAGCTT <u>G</u> CTCATTATTGCCGAGATAATG
H282Nf	ATACAAGCTT <u>G</u> G <u>C</u> T <u>A</u> TTATTGCCGAGATAATGGTCTAC
A281S_H282Nf	ATACAAGCTT <u>G</u> T <u>C</u> <u>A</u> TTATTGCCGAGATAATGGTCTAC
C449Gr	AGATGCCGCCGCTAGTCCGGGCTCCATTGCC <u>A</u> GCTCGCGAATAATT
K429Qf	CTAGAAGCATGTGT <u>A</u> AGCTCGTAATGAAG
K429Qr	CTTCATTACGAGCTT <u>G</u> TACACATGCTTCTAG